Parity-violating nucleon-nucleon interaction from different approaches

B. Desplanques,[1,*] C. H. Hyun,[2,†] S. Ando,[2,‡] and C.-P. Liu[3,§]

[1]*LPSC, Université Joseph Fourier Grenoble 1, CNRS/IN2P3, INPG, F-38026 Grenoble Cedex, France*

[2]*Department of Physics and Institute of Basic Science, Sungkyunkwan University, Suwon 440-746, Korea*

[3]*T-16, Theoretical Division, Los Alamos National Laboratory, Los Alamos, New Mexico 87545, USA*

(Received 13 March 2008; published 11 June 2008)

Two-pion exchange parity-violating nucleon-nucleon interactions from recent effective field theories and earlier fully covariant approaches are investigated. The potentials are compared with the goal of obtaining better insight into the role of low-energy constants appearing in the effective field theory approach and its convergence in terms of a perturbative series. The results are illustrated by considering the longitudinal asymmetry of polarized protons scattering off protons, $\vec{p} + p \to p + p$, and the asymmetry of the photon emission in radiative capture of polarized neutrons by protons, $\vec{n} + p \to d + \gamma$.

DOI: 10.1103/PhysRevC.77.064002 PACS number(s): 13.75.Cs

I. INTRODUCTION

Effective field theory (EFT) underlies most recent developments in the domain of the nucleon-nucleon (NN) strong interaction [1–4]. The approach is mainly motivated by the fact that a large part of the short-range interaction is essentially unknown. Its detailed description may not be really relevant at low energy and a schematic one, represented by contact interactions with low-energy constants (LECs), could be sufficient. Moreover, such an approach could account for important properties in relation to QCD dynamics (i.e., chiral symmetry). Implementing these properties can be done with chiral perturbation theory [5]. One is thus led to distinguish contributions at different orders. Beyond the one-pion exchange (OPE), which appears at leading order (LO), two-pion exchange (TPE), which is relevant at next-to-next-to-leading order (NNLO), has been considered.[1] Higher order terms are also considered, contributing to a successful description of the strong interaction.

Naturally, the EFT approach has been applied to the weak, parity-violating (PV) NN interaction [6], superposing on earlier phenomenological works in the 1970s [7–9] a systematic perturbation scheme in terms of an expansion parameter characterizing the theory. Thus, a one-pion-exchange contribution appears at LO whereas the two-pion-exchange contribution is part of those at NNLO. It was claimed that effects from the TPE contribution could be potentially large. Estimates have been made for various observables [10,11] and, although they do not contradict this expectation, they have evidenced a large range of uncertainty [10]. This points to the role of a contact term present in the operators, which has to be completed in any case by a LEC contribution and cannot be therefore considered as physically relevant by itself. The PV TPE contribution was considered in the 1970s in several works, starting from a covariant formalism and based on Feynman diagrams [12] or dispersion relations [13–15]. Originally, these works were motivated by the expectation that the TPE could play a role in the PV case as important as in the strong interaction one, but this was actually disproved by the studies. A similar motivation has recently been addressed within the EFT approach with some attention to the contribution involving the Δ excitation [16] (see also Refs. [17,18] with regard to this last respect). Interestingly, the TPE contribution in various processes turned out to be well determined but rather small [13,15,19] and, in particular, unessential in comparison with other uncertainties (PV couplings constants, nuclear-structure description, etc.). This last feature largely explains its omission in later works. In view of different conclusions, we believe that a comparison of both the recent and earlier works is useful. Some preliminary results were presented in Ref. [20].

These studies could be relevant because, in contrast to the strong interaction, it is not possible to determine at present the LECs owing to the lack of sufficient and accurate enough experimental data. On the one hand, they could tell us about the role of contact interactions in making the two approaches as close as possible. The contributions of these contact interactions can be ascribed to the LEC or the "finite" range part, depending on the subtraction scheme. On the other hand, they could provide information on the convergence of the perturbative expansion of the potential in the EFT approach, which is limited to NNLO so far. In the field of the strong NN interaction [21] or weak semi-leptonic interactions [22], there are hints for non-negligible corrections.

The plan of this paper is as follows. In Sec. II, results relative to the TPE contribution from a covariant approach are recalled (isovector part). All components of this interaction and their convergence properties in particular are discussed. Section III is devoted to results in the EFT approach, completed by those obtained from the contribution of time-ordered

*desplanq@lpsc.in2p3.fr

†hch@color.skku.ac.kr; now at Department of Physics Education, Daegu University, Gyeongsan 712-714, Korea.

‡Shung-ichi.Ando@manchester.ac.uk; now at Theoretical Physics Group, School of Physics and Astronomy, The Manchester University, Manchester M13 9PL, United Kingdom.

§cliu38@wisc.edu; now at Department of Physics, University of Wisconsin-Madison, 1150 University Avenue, Madison, Wisconsin 53706-1390, USA.

[1]There are different conventions to denote orders. We use the one in agreement with what has been used in the parity-violating case.

diagrams as a check. In Sec. IV, we examine similarities and differences between results of these approaches and those from an expansion of the covariant one at the lowest nonzero order in the inverse of the nucleon mass, $1/M$. A numerical comparison concerning a few aspects of potentials so obtained is given in Sec. V. Estimates of the effects in two selected processes, proton-proton scattering and radiative neutron-proton capture at thermal energy, are finally given in Sec. VI. These two processes allow one to illustrate the two types of PV effects that are expected from the TPE interaction at low energy. Section VII contains the conclusion. This is completed by appendices concerning the removing of the iterated OPE and the EFT approach.

II. TWO-PION EXCHANGE FROM A COVARIANT FORMALISM

We consider here the isovector PV TPE contribution to the NN interaction obtained from a fully covariant formalism. It is induced by an elementary PV pion-nucleon coupling, most often denoted by h_π^1. As this coupling also determines the strength of the PV OPE interaction, we give the corresponding expression in terms of both the momentum transfer, $\vec{q}$, and the relative momenta, $\vec{p}$ and $\vec{p}'$:

$$V_\pi(\vec{q}) = \frac{ig_{\pi NN}h_\pi^1}{2\sqrt{2}M}(\vec{\tau}_1\times\vec{\tau}_2)^z\frac{(\vec{\sigma}_1+\vec{\sigma}_2)\cdot(\vec{p}'-\vec{p})}{m_\pi^2+q^2} = -\frac{ig_{\pi NN}h_\pi^1}{2\sqrt{2}M}(\vec{\tau}_1\times\vec{\tau}_2)^z\frac{(\vec{\sigma}_1+\vec{\sigma}_2)\cdot\vec{q}}{m_\pi^2+q^2}. \quad (1)$$

Because of possible ambiguity, we further specify the notation for momenta:

$$\vec{p} = \tfrac{1}{2}(\vec{p}_1-\vec{p}_2), \quad \vec{p}' = \tfrac{1}{2}(\vec{p}_1'-\vec{p}_2'), \quad \vec{q} = (\vec{p}_1-\vec{p}_1') = -(\vec{p}_2-\vec{p}_2') = (\vec{p}-\vec{p}'), \quad (2)$$

where the primed and nonprimed momenta refer to those of particles appearing, respectively, in the bra and ket states. In configuration space, the interaction thus recovers its standard form

$$V_\pi(\vec{r}) = \frac{ig_{\pi NN}h_\pi^1}{2\sqrt{2}M}(\vec{\tau}_1\times\vec{\tau}_2)^z(\vec{\sigma}_1+\vec{\sigma}_2)\cdot\left[\vec{p},\frac{e^{-m_\pi r}}{4\pi r}\right] = -\frac{g_{\pi NN}h_\pi^1}{2\sqrt{2}M}(\vec{\tau}_1\times\vec{\tau}_2)^z(\vec{\sigma}_1+\vec{\sigma}_2)\cdot(\vec{r}_1-\vec{r}_2) \times\frac{e^{-m_\pi r}(1+m_\pi r)}{4\pi r^3}, \quad (3)$$

with $r = |\vec{r}_1-\vec{r}_2|$. The first studies of the isovector PV TPE contribution were made in the early 1970s [12–15], being partially motivated by the underestimation of some observed PV effects using the standard PV NN interaction available at that time. Similarly to the strong-interaction case, where the TPE contribution is quantitatively more important than the OPE one, it was believed that the TPE contribution could also play an essential role in the PV case.

Various studies roughly agree with each other, after mistakes are corrected in some cases [12,14]. Differences involve in particular the formalism (calculations using Feynman diagrams or dispersion relations), nonrelativistic approximations in external nucleon lines, or the removal of the OPE-iterated contribution in the box diagram. The choice of the Green's function in the last ingredient was rather unimportant owing to the introduction of cutoffs in applications. It could however be important in unrestricted calculations. The point is of relevance with respect to a comment made in Ref. [6] about the absence of convergence in earlier calculations. It will be discussed in more detail in the following when expressions for the TPE contribution are given.

The crossed and noncrossed box diagrams that enter the isovector TPE contribution of interest here are represented in Fig. 1, where the intermediate hadron on the upper line can be a nucleon as well as a resonance [$\Delta(1232)$, $N^*(1440)$, or $N^*(1518)$]. For our purpose and also for simplicity, we only retain the nucleon. Altogether, the corresponding contribution to the isovector interaction involves six different terms. Following the notation of Ref. [15], we can write it quite generally in momentum space as

$$\begin{aligned} V(\vec{p}',\vec{p}) &= V_{44}+V_{34}+V_{56}+V_{75}+V_{66}+V_{85} \\ &= i(\vec{\tau}_1+\vec{\tau}_2)^z(\vec{\sigma}_1\times\vec{\sigma}_2)\cdot(\vec{p}'-\vec{p})v_{44}(q,\ldots) \\ &\quad +(\vec{\tau}_1+\vec{\tau}_2)^z(\vec{\sigma}_1-\vec{\sigma}_2)\cdot(\vec{p}'+\vec{p})v_{34}(q,\ldots) \\ &\quad +i(\vec{\tau}_1\times\vec{\tau}_2)^z(\vec{\sigma}_1+\vec{\sigma}_2)\cdot(\vec{p}'-\vec{p})v_{56}(q,\ldots) \\ &\quad +(\vec{\tau}_1-\vec{\tau}_2)^z(\vec{\sigma}_1+\vec{\sigma}_2)\cdot(\vec{p}'+\vec{p})v_{75}(q,\ldots) \\ &\quad +(\vec{\tau}_1\times\vec{\tau}_2)^z[\vec{\sigma}_1\cdot\vec{q}\vec{\sigma}_2\cdot(\vec{p}'+\vec{p})\times\vec{q} \\ &\quad +(\vec{\sigma}_1\leftrightarrow\vec{\sigma}_2)]v_{66}(q,\ldots) \end{aligned}$$

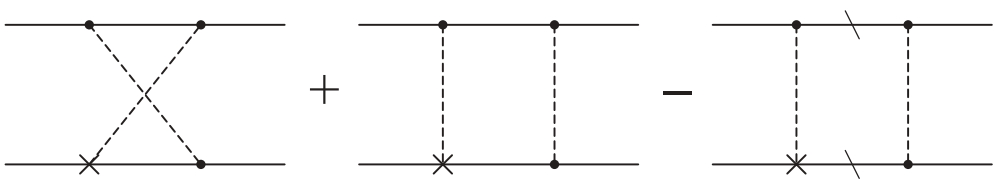

FIG. 1. Two-pion exchange in the covariant approach: These diagrams represent the contributions of the crossed box, the noncrossed box, and the iterated OPE that has to be subtracted from the previous one. The continuous line represents a baryon and the dashed one a pion. The contributions with nucleon and nucleon resonances in the intermediate state have been considered in the literature. Only the first one is retained here but the role of the other ones will also be mentioned. The PV meson-nucleon vertex is marked with a cross (×). The last diagram on the right represents the iterated OPE, with the backslash indicating that the corresponding nucleon is on-mass shell. Further diagrams with a different order of the parity-violating and parity-conserving meson-nucleon vertices on the same nucleon line (not shown here) are also considered.

$$- i(\vec{\tau}_1 - \vec{\tau}_2)^z [\vec{\sigma}_1 \cdot (\vec{p}' + \vec{p})\vec{\sigma}_2 \cdot (\vec{p}' + \vec{p}) \times \vec{q} + (\vec{\sigma}_1 \leftrightarrow \vec{\sigma}_2)] v_{85}(q, \ldots). \quad (4)$$

Functions $v_{ij}(q, \ldots)$ assume a dispersion-relation form

$$v_{ij}^{\mathrm{COV}}(q, \ldots) = \frac{1}{\pi} \int_{4m_\pi^2}^{\infty} dt' \frac{g_{ij}(t', \ldots)}{\sqrt{t'}(t' + q^2)}, \quad (5)$$

and dots represent possible extra dependence on $\vec{p}'$ and $\vec{p}$ (kinetic energy in particular).

The configuration-space PV TPE potential is obtained from the standard relation

$$v(r) = \int \frac{d\vec{q}}{(2\pi)^3} e^{-i\vec{q}\cdot\vec{r}} v(q). \quad (6)$$

Its expression thus reads

$$\begin{aligned} V(r, \vec{p}', \vec{p}) &= i(\vec{\tau}_1 + \vec{\tau}_2)^z (\vec{\sigma}_1 \times \vec{\sigma}_2) \cdot [\vec{p}, v_{44}(r, \ldots)] \\ &+ (\vec{\tau}_1 + \vec{\tau}_2)^z (\vec{\sigma}_1 - \vec{\sigma}_2) \cdot \{\vec{p}, v_{34}(r, \ldots)\} \\ &+ i(\vec{\tau}_1 \times \vec{\tau}_2)^z (\vec{\sigma}_1 + \vec{\sigma}_2) \cdot [\vec{p}, v_{56}(r, \ldots)] \\ &+ (\vec{\tau}_1 - \vec{\tau}_2)^z (\vec{\sigma}_1 + \vec{\sigma}_2) \cdot \{\vec{p}, v_{75}(r, \ldots)\} \\ &+ 2i(\vec{\tau}_1 \times \vec{\tau}_2)^z \left(\vec{\sigma}_1 \cdot \left[\vec{p}, \vec{\sigma}_2 \cdot \vec{l} \frac{1}{r} \frac{d}{dr} v_{66}(r, \ldots) \right] \right. \\ &\left. + (\vec{\sigma}_1 \leftrightarrow \vec{\sigma}_2) \right) - 2(\vec{\tau}_1 - \vec{\tau}_2)^z \\ &\times \left(\vec{\sigma}_1 \cdot \left\{ \vec{p}, \vec{\sigma}_2 \cdot \vec{l} \frac{1}{r} \frac{d}{dr} v_{85}(r, \ldots) \right\} + (\vec{\sigma}_1 \leftrightarrow \vec{\sigma}_2) \right), \end{aligned} \quad (7)$$

where $\vec{l} = \vec{r} \times \vec{p}$ and

$$v_{ij}^{\mathrm{COV}}(r, \ldots) = \frac{1}{4\pi^2} \int_{4m_\pi^2}^{\infty} dt' g_{ij}(t', \ldots) \frac{e^{-r\sqrt{t'}}}{r\sqrt{t'}} \quad (8)$$

and $\vec{p}'$ and $\vec{p}$, which dots account for, now have an operator character and should be placed, respectively, on the left and the right, in accordance with our conventions.

The terms V_{44}, V_{34}, V_{56}, and V_{75} appear at the first order in a p/M expansion of the Lorentz invariants appearing in the expression of the interaction. The two other terms, V_{66} and V_{85}, appear at the third order in p/M. They can therefore be considered as relativistic corrections. Moreover, they only contribute when going beyond the transitions between lowest partial wave states (i.e., S to P), which generally dominate at low energy (where most PV data are available). For these two reasons, the corresponding terms were discarded in the past, which we also do here. We however stress that these higher order terms are necessary to get a full mapping of the NN interaction, especially to discriminate transitions involving higher partial waves such as ${}^3P_1$–${}^3D_1$ and ${}^3P_2$–${}^3D_2$, ${}^3D_2$–${}^3F_2$ and ${}^3D_3$–${}^3F_3$, etc. It is also noticed that this nonrelativistic expansion only involves the nucleon external lines, as done in other approaches. No expansion is made for internal nucleon lines where big effects could arise. As our results presented in this paper only retain part of the full relativistic structure, they will be denoted "covariant" to avoid overstating this property.

We now consider the expressions of the V_{44}, V_{34}, V_{56}, and V_{75} terms. It is first noticed that V_{44} and V_{34} only receive contributions from the crossed diagram whereas V_{56} and V_{75} also get some from the noncrossed one. In this case, one therefore has to worry about the removal of the iterated OPE and, especially, about the choice of the Green's function that enters the calculation. In Ref. [13], the Green's function $(2E_0 - 2E)^{-1}$ was used, by taking into account that the Schrödinger equation is linear in the energy of the system, E_0, and assuming moreover that the kinetic energy of particles retains its relativistic form ($E = \sqrt{M^2 + p^2}$ in the c.m. frame). In later works [14,15], a Green's function more in agreement with a nonrelativistic Schrödinger equation, $E/(p_0^2 - p^2)$, was instead used. The difference, a factor of $2E/(E_0 + E)$, had minor numerical effects in the past calculations where cutoffs were introduced in the dispersion integrals [Eq. (5)]. The difference however matters in unrestricted calculations. Dispersion-relation integrals diverge in the first case but they converge in the second one. The corresponding Green's function for the latter case can be written in the form $E/(E_0^2 - E^2)$, which rather evokes an equation with a quadratic-mass operator. Such an equation is known to provide solutions with a behavior in the relativistic domain better than the linear one [23]. This is the choice made here. Taking into account that the kinetic-energy dependence is small and that we are interested in low-energy processes, we can set the momentum in functions $g(q, \ldots)$ to 0. In a similar way as Ref. [13] (with details given in Appendix A1), the closed expressions for these functions are then obtained. If we omit dots (which are no longer justified), they read

$$\begin{aligned} g_{44}(t') &= \tilde{K} \frac{1}{2M} \left[\frac{4q_\pi}{\chi^2} + \frac{H}{M^2} - G \left(\frac{1}{M^2} + \frac{1}{\chi^2} \right) \right], \\ g_{34}(t') &= \tilde{K} \frac{1}{2M^3} \left(G - \frac{Hx^2}{x^2 + 4M^2 q_\pi^2} \right), \\ g_{56}(t') &= -\tilde{K} \frac{1}{2M} \frac{Hx}{x^2 + 4M^2 q_\pi^2} - \tilde{K} \frac{x}{M^2 m_\pi^2} \arctan \left(\frac{m_\pi^2}{2Mq_\pi} \right) \\ &+ \tilde{K} \int_{k_-^2}^{k_+^2} \frac{dk^2}{\sqrt{k^2 t' - \left(m_\pi^2 + k^2\right)^2}} \frac{1}{2E(E + M)} \\ &\times \left(\frac{x}{M^2} + \frac{k^2}{M(E + M)} \right), \\ g_{75}(t') &= \tilde{K} \frac{4x^2}{M^2 m_\pi^2 t'} \arctan \left(\frac{m_\pi^2}{2Mq_\pi} \right) + \tilde{K} \frac{2G}{Mt'} \\ &- \tilde{K} \int_{k_-^2}^{k_+^2} \frac{dk^2}{\sqrt{k^2 t' - \left(m_\pi^2 + k^2\right)^2}} \frac{2}{E(E + M)} \\ &\times \left(\frac{x^2}{M^2 t'} + \frac{2Ex}{Mt'} - \frac{k^2}{M(E + M)} \right. \\ &\left. - \frac{k^4}{M(E + M)t'} \right), \end{aligned} \quad (9)$$

where

$$\tilde{K} = \frac{g_{\pi NN}^3 h_\pi^1}{32\pi\sqrt{2}}, \quad q_\pi = \sqrt{\frac{t'}{4} - m_\pi^2},$$
$$\chi^2 = M^2 - \frac{t'}{4}, \quad x = \frac{t'}{2} - m_\pi^2,$$

$$
\begin{aligned}
H &= 2\sqrt{\frac{x^2+4M^2q_\pi^2}{t'}}\ln\left(\frac{\sqrt{x^2+4M^2q_\pi^2}+q_\pi\sqrt{t'}}{\sqrt{x^2+4M^2q_\pi^2}-q_\pi\sqrt{t'}}\right),\\
G &= \frac{2x}{\chi}\arctan\left(\frac{2q_\pi\chi}{x}\right)\ [\text{for, } \chi^2\geqslant 0],\\
&= \frac{x}{\sqrt{-\chi^2}}\ln\left(\frac{x+2q_\pi\sqrt{-\chi^2}}{x-2q_\pi\sqrt{-\chi^2}}\right)\ [\text{for, } \chi^2\leqslant 0],\\
k_\pm^2 &= x\pm q_\pi\sqrt{t'},\quad E=\sqrt{M^2+k^2}.
\end{aligned}
\tag{10}
$$

Looking at the asymptotic behavior of the functions $g_{ij}(t')$ for large t', we notice that the dominant contributions of individual terms, $\propto t'^{1/2}$, as well as the constant ones, cancel (see Appendix A2 for details). One is thus left with the following contributions:

$$
\begin{aligned}
g_{44}(t')_{t'\to\infty} &= \tilde{K}\frac{2}{M\sqrt{t'}}\left[\ln\left(\frac{t'}{M^2}\right)-1\right],\\
g_{34}(t')_{t'\to\infty} &= \tilde{K}\frac{2}{M\sqrt{t'}}\left[\ln\left(\frac{t'}{M^2}\right)-1\right],\\
g_{56}(t')_{t'\to\infty} &= -\tilde{K}\frac{1}{M\sqrt{t'}}\left[\frac{5}{8}\ln\left(\frac{t'}{M^2}\right)+\frac{15}{8}-\frac{3}{2}\ln(2)\right],\\
g_{75}(t')_{t'\to\infty} &= \tilde{K}\frac{1}{M\sqrt{t'}}\left[\frac{9}{4}\ln\left(\frac{t'}{M^2}\right)-\frac{1}{4}+\ln(2)\right].
\end{aligned}
\tag{11}
$$

In all cases, the functions $g_{ij}(t')$ behave asymptotically as $t'^{-1/2}$, up to log terms, ensuring the convergence of the integrals given in Eq. (5). This result is important as it allows one to consider the dispersion approach as a benchmark, thus providing information about contributions that are ascribed to LECs as well as possible higher order corrections in other approaches.

III. TWO-PION EXCHANGE FROM THE EFT APPROACH

A. EFT approach

The PV TPE at NNLO has been calculated in the EFT approach by Zhu *et al.* [6]. It contains two components that involve functions $\tilde{C}_2^{2\pi}(q)$ and $C_6^{2\pi}(q)$ and correspond here to the components V_{44} and V_{56} of the more complete interaction given by Eq. (4). The contributions being accounted for correspond to the diagrams shown in Fig. 2. Their expressions for the finite-range part and the associated contact term have been obtained in the maximal-subtraction (MX) scheme. By factoring out the spin-isospin dependence and taking into account corrections made since then [10], they read[2]

$$
\begin{aligned}
v_{44}^{\text{EFT}}(q) &= -4\sqrt{2}\pi\frac{h_\pi^1}{\Lambda_\chi^3}\left(g_A^3L(q)\right),\\
v_{56}^{\text{EFT}}(q) &= -\sqrt{2}\pi\frac{h_\pi^1}{\Lambda_\chi^3}\left(g_AL(q)-g_A^3\left(3L(q)-H(q)\right)\right),
\end{aligned}
\tag{12}
$$

where the scale Λ_χ is roughly given by $\Lambda_\chi = 4\pi f_\pi \simeq 4\pi g_A M/g_{\pi NN} \simeq 1$ GeV and the $L(q)$ and $H(q)$ functions are defined as

$$
\begin{aligned}
L(q) &= \frac{\sqrt{q^2+4m_\pi^2}}{q}\ln\left(\frac{\sqrt{q^2+4m_\pi^2}+q}{2m_\pi}\right)\\
&= \frac{\sqrt{q^2+4m_\pi^2}}{2q}\ln\left(\frac{\sqrt{q^2+4m_\pi^2}+q}{\sqrt{q^2+4m_\pi^2}-q}\right),\\
H(q) &= \frac{4m_\pi^2}{q^2+4m_\pi^2}L(q).
\end{aligned}
\tag{13}
$$

The details of the contributions corresponding to diagrams (b), (c), and (d) in Fig. 2 can be found in Appendix B. The terms entering the interaction should be completed by contact terms

$$
\begin{aligned}
v_{44}^{\text{CT}} &= C_{44},\\
v_{56}^{\text{CT}} &= C_{56}.
\end{aligned}
\tag{14}
$$

The contributions from TPE to these contact terms are also given in Appendix B, where it is seen that they require some renormalization. The sum of the EFT TPE and contact contributions should be well determined, but how it is split between the two terms is not. In the minimal-subtraction ($\overline{\text{MS}}$) scheme,[3] the part of the contact term that is proportional to $1+\ln(\mu/m_\pi)$ (see Appendix B) is shifted to the EFT TPE part. In such a case, the term "1" cancels the function $L(q)$ at $q=0$ and the log term, for $\mu \geqslant m_\pi$, changes the overall sign of the potential in the low-q range.

B. Relation to the time-ordered-diagram approach

When integrating the EFT expressions of the TPE interaction over the time component of the integration variable entering some loop, it is expected that one should recover expressions obtained from considering time-ordered (TO) diagrams in the nonrelativistic limit ($\vec{v}\to 0$, where $\vec{v}$ is the nucleon velocity $\vec{v}\simeq\vec{p}/M$). As this check was quite useful in determining the correct expressions given in the previous section, we give in the following the raw expressions obtained from the contribution of these time-ordered diagrams, which are shown in Fig. 3. Starting from the elementary πNN interaction, $g_{\pi NN}\vec{\sigma}\cdot\vec{k}/(2M\sqrt{\omega_k})$ (with $\omega_k=\sqrt{m_\pi^2+k^2}$), one gets

$$
\begin{aligned}
v_{44}^{\text{TO}}(q) = \frac{g_{\pi NN}^3h_\pi^1}{4\sqrt{2}M^3}\int\frac{d\vec{k}}{(2\pi)^3}\frac{k^2-(\vec{k}\cdot\hat{q})^2}{\omega_i\omega_j}\left(\frac{1}{\omega_i^2(\omega_i+\omega_j)}\right.\\
\left.+\frac{1}{(\omega_i+\omega_j)\omega_j^2}+\frac{1}{\omega_i(\omega_i+\omega_j)\omega_j}\right),
\end{aligned}
$$

[2] We have followed our own conventions, as the conventions used to present the final results in Ref. [6] differ from that ones defined by the same authors at an earlier stage.

[3] The scheme we denoted by MN in a previous work [10] actually corresponds to the $\overline{\text{MS}}$ scheme, so we change the name as adopted here.

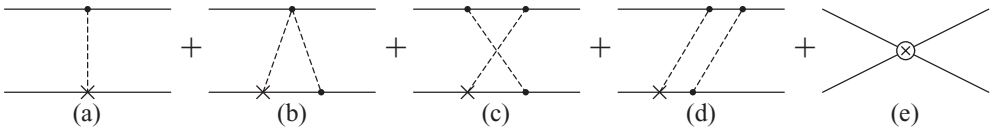

FIG. 2. One- and two-pion exchange in the EFT approach showing the contributions from the OPE (a), from the triangle TPE (b), from the crossed TPE (c), from the noncrossed TPE (d), and from the contact term (e). See the caption of Fig. 1 for further comments.

$$v_{56}^{\mathrm{TO}}(q) = \frac{g_{\pi NN}^3 h_\pi^1}{4\sqrt{2}M^3}\left[\frac{1}{2}\int \frac{d\vec{k}}{(2\pi)^3}\frac{1}{\omega_i\omega_j(\omega_i+\omega_j)} - \frac{1}{2}\int \frac{d\vec{k}}{(2\pi)^3}\frac{k^2-\frac{q^2}{4}}{\omega_i\omega_j}\left(\frac{1}{\omega_i^2(\omega_i+\omega_j)} + \frac{1}{(\omega_i+\omega_j)\omega_j^2} + \frac{1}{\omega_i(\omega_i+\omega_j)\omega_j}\right)\right], \tag{15}$$

where $\omega_i = \sqrt{m_\pi^2 + (\vec{k}+\vec{q}/2)^2}$ and $\omega_j = \sqrt{m_\pi^2 + (\vec{k}-\vec{q}/2)^2}$. The three integrals involve the contributions successively from the crossed diagrams (the first line of Fig. 3), Z-type ones (the second line of Fig. 3), and both crossed and noncrossed diagrams (the first and third lines of Fig. 3). The Z-type diagrams are calculated by assuming a pseudo-scalar coupling, consistently with the dispersion-relation approach used independently, and retaining the lowest nonzero term in a $1/M$ expansion. As is known, the contribution alone violates chiral symmetry (see, for instance, Ref. [24]). The expected symmetry is restored by further contributions, which can be calculated in the same formalism (see details in Sec. IV B). Contributions of all diagrams in Fig. 3 diverge but they contain a well-defined part that can be analytically calculated. Interestingly, the expressions so obtained can be cast into the form of dispersion integrals. This property stems from considering a complete set of topologically equivalent time-ordered diagrams. This writing is interesting as it greatly facilitates the comparison with the expressions obtained from a covariant approach, which evidences the same form. It is thus found that the different integrals in Eqs. (15) read

$$\begin{aligned}
&\int d\vec{k}\frac{k^2-(\vec{k}\cdot\hat{q})^2}{\omega_i\omega_j}\left(\frac{1}{\omega_i^2(\omega_i+\omega_j)} + \frac{1}{(\omega_i+\omega_j)\omega_j^2} + \frac{1}{\omega_i(\omega_i+\omega_j)\omega_j}\right)\\
&\quad = 4\pi(1-L(q)) + \int d\vec{k}\frac{k^2}{\omega_k^5} = \pi\int_{4m_\pi^2}^{\infty} dt'\frac{2\sqrt{t'-4m_\pi^2}}{\sqrt{t'}(t'+q^2)},\\
&\int d\vec{k}\frac{1}{\omega_i\omega_j(\omega_i+\omega_j)}\\
&\quad = 2\pi(1-L(q)) + \frac{1}{2}\int d\vec{k}\frac{1}{\omega_k^3} = \pi\int_{4m_\pi^2}^{\infty} dt'\frac{\sqrt{t'-4m_\pi^2}}{\sqrt{t'}(t'+q^2)},\\
&\int d\vec{k}\frac{k^2-\frac{q^2}{4}}{\omega_i\omega_j}\left(\frac{1}{\omega_i^2(\omega_i+\omega_j)} + \frac{1}{(\omega_i+\omega_j)\omega_j^2} + \frac{1}{\omega_i(\omega_i+\omega_j)\omega_j}\right)\\
&\quad = 2\pi(3(1-L(q)) + H(q)) + \frac{3}{2}\int d\vec{k}\frac{k^2}{\omega_k^5}\\
&\quad = \pi\int_{4m_\pi^2}^{\infty} dt'\frac{3(t'-4m_\pi^2)+4m_\pi^2}{\sqrt{t'}\sqrt{t'-4m_\pi^2}(t'+q^2)}.
\end{aligned} \tag{16}$$

Owing to the divergent character of these integrals, these equalities hold up to some constant. This does not however affect the q^2-dependent part. One can thus remove an infinite contribution so that the interaction takes a definite value at

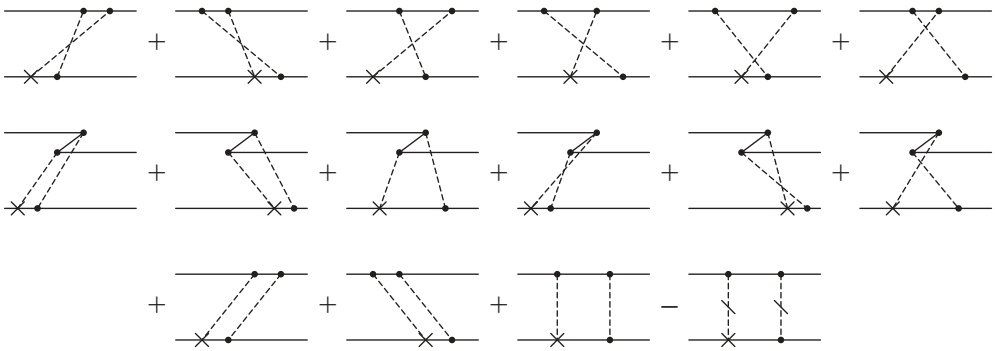

FIG. 3. Two-pion exchange in the time-ordered diagram approach showing the contributions from the crossed diagrams (the first line), from the Z-type contributions (the second line, identified as triangle diagrams in a different approach), and from the noncrossed diagrams (the diagrams on the third line). The last two diagrams differ in that the first of them involves a meson propagator with off-energy shell contributions, which are omitted in the other one (indicated by a backslash on the meson lines). This last contribution, which arises from the iterated OPE, has to be subtracted from the previous one. The discrepancy involves a factor $E_0 - k^2/M$, which cancels a similar factor entering the denominator of the Green function (where $\vec{k}$ can be identified as the loop momentum). See the caption of Fig. 1 for further comments.

some q^2. A particularly interesting choice is to subtract a part so that the remaining one, which contains the most physically relevant part, cancels at $q^2 = 0$. By looking at this quantity, one can usefully compare different approaches. To some extent the slope with respect to q^2 at $q^2 = 0$ provides information on the sign and the strength of the interaction at finite distances. The $L(q)$ function in these equalities thus points to a configuration-space interaction with an opposite sign at finite distances. The divergent part is not without interest however. It tells us in which direction the (short-range) subtracted interaction is likely to contribute. By integrating out the contribution $t' \geqslant \tilde{\Lambda}^2$ on the right-hand side of Eqs. (16) in the small-q limit, one successively gets the approximate factors $4\pi \ln(\tilde{\Lambda}/2m_\pi)$, $2\pi \ln(\tilde{\Lambda}/2m_\pi)$, and $6\pi \ln(\tilde{\Lambda}/2m_\pi)$. This suggests two observations. On the one hand, for large enough $\tilde{\Lambda}$, the right-hand side has a sign opposite to that given by the $L(q)$ term at the left-hand side, confirming the observation in configuration space. On the other hand, this factor allows one to make some relation with the EFT interaction calculated in the minimal-subtraction scheme, which involves similar log terms (with $\tilde{\Lambda}$ replaced by μ).

Comparing these expressions, Eqs. (16), with the previous EFT ones, Eqs. (12), we find that the q^2 dependencies are very similar. By assuming the choice $\Lambda_\chi = 4\pi g_A M/g_{\pi NN}$, an identity is actually found for the potential, $v_{44}(q)$, as well as the second term for the other potential, $v_{56}(q)$. For the first term in $v_{56}(q)$, which can be associated with a triangle-type diagram, the time-ordered diagram approach used here gives a factor g_A^3 instead of g_A as directly obtained from the Weinberg-Tomozawa term. This discrepancy points to the fact that the approach misses some contribution. As already mentioned, this will be discussed in more detail in Sec. IV B when making a comparison with the expressions obtained from the covariant formalism.

IV. RELATION OF THE EFT APPROACH TO THE COVARIANT ONE

We discuss here similarities and differences between the expressions obtained from the full covariant approach and the EFT one presented in Secs. II and III, respectively.

A. Similarities (large-M limit)

To make a comparison of the EFT and time-ordered-diagram approaches with the covariant one, the first step is to derive expressions in the large-M limit for the last case. Taking this limit in the simplest minded way for the H and G functions given in Eq. (10), one gets

$$\begin{aligned} H_{M\to\infty} &= 4q_\pi = 2\sqrt{t' - 4m_\pi^2}, \\ G_{M\to\infty} &= \frac{(t' - 2m_\pi^2)}{M}\left(\frac{\pi}{2} - \frac{x}{2q_\pi M}\right) \simeq \pi\frac{x}{M}. \end{aligned} \tag{17}$$

Inserting these limits in Eqs. (9), one finds

$$g_{44}(t')_{M\to\infty} = \tilde{K}\frac{4q_\pi}{M^3} = \tilde{K}\frac{2\sqrt{t' - 4m_\pi^2}}{M^3},$$

$$\begin{aligned} g_{34}(t')_{M\to\infty} &= \tilde{K}\frac{\pi}{M^4}\frac{x}{2} = \tilde{K}\frac{\pi}{M^4}\frac{t' - 2m_\pi^2}{4}, \\ g_{56}(t')_{M\to\infty} &= -\tilde{K}\frac{x}{q_\pi M^3} = -\tilde{K}\frac{(t' - 2m_\pi^2)}{M^3\sqrt{t' - 4m_\pi^2}}, \\ g_{75}(t')_{M\to\infty} &= \tilde{K}\frac{\pi}{M^4}\left(\frac{t' - 4m_\pi^2}{16} + \frac{3}{2}\frac{t' - 2m_\pi^2}{4}\right). \end{aligned} \tag{18}$$

In obtaining these expressions, one has taken into account that the integral in Eq. (9) for $g_{56}(t')$ has a higher $1/M$ order ($1/M^4$). The case of $g_{75}(t')$ is more complicated as individual contributions of $1/M^2$ and $1/M^3$ order cancel. In any case, we notice that the large-M limit does not commute with the large-t' limit [compare with the results given in Eq. (11)]. Differences from the "covariant" results are therefore expected when considering short distances, where the last limit is relevant. The insertion of these limits in the dispersion-relation integrals, Eqs. (5), allows one to recover the expressions of the time-ordered-diagram approach at the lowest order, $1/M^3$, for interactions V_{44} and V_{56}:

$$\begin{aligned} v_{44}(q)_{M\to\infty} &= \frac{g_{\pi NN}^3 h_\pi^1}{16\sqrt{2}\pi^2 M^3}\int_{4m_\pi^2}^{\infty} dt' \frac{\sqrt{t' - 4m_\pi^2}}{\sqrt{t'}(t' + q^2)}, \\ v_{56}(q)_{M\to\infty} &= -\frac{g_{\pi NN}^3 h_\pi^1}{32\sqrt{2}\pi^2 M^3}\int_{4m_\pi^2}^{\infty} dt' \frac{(t' - 2m_\pi^2)}{\sqrt{t'}\sqrt{t' - 4m_\pi^2}(t' + q^2)}. \end{aligned} \tag{19}$$

For the interaction V_{56}, it is noticed that the two terms involving integrands proportional to $-(t' - 4m_\pi^2)$ and $3(t' - 4m_\pi^2) + 4m_\pi^2$ in Eq. (15) [together with Eq. (16)] combine to give the factor proportional to $(t' - 2m_\pi^2)$ appearing in the large-M-limit expression of $g_{56}(t')$, Eq. (18).

Expressions for both V_{44} and V_{56} can be cast into a form that facilitates the comparison with Zhu *et al.*'s work [6]. In this order, a factor $g_{\pi NN}^3/(4\pi g_A M)^3$, which can be identified as the $1/\Lambda_\chi^3$ factor in their work, is partly factored out. One ascribes the infinities present in the dispersion integrals temporarily to LECs, knowing that these ones should be finite in practice. We thus have

$$\begin{aligned} v_{44}(q)_{M\to\infty} &= v_{44}^{\mathrm{LM}}(q) + C'_{44}, \\ v_{56}(q)_{M\to\infty} &= v_{56}^{\mathrm{LM}}(q) + C'_{56}, \end{aligned}$$

with

$$\begin{aligned} v_{44}^{\mathrm{LM}}(q) &= -4\sqrt{2}\pi\frac{g_{\pi NN}^3 h_\pi^1}{(4\pi g_A M)^3} g_A^3 L(q), \\ v_{56}^{\mathrm{LM}}(q) &= -\sqrt{2}\pi\frac{g_{\pi NN}^3 h_\pi^1}{(4\pi g_A M)^3}\big(g_A^3 L(q) - g_A^3(3L(q) - H(q))\big). \end{aligned} \tag{20}$$

The only significant discrepancy with Zhu *et al.*'s work, Eqs. (12), concerns the first term of V_{56}, which contains a factor g_A^3 instead of g_A, confirming the observation already made in the time-ordered-diagram approach.

B. Differences

After having shown how the expressions of the EFT (or the time-ordered-diagram) approach can be obtained from the

covariant ones for the gross features, we now examine the differences.

The first difference concerns the convergence properties of the integral expressions for the potentials $v_{ij}(q)$, Eqs. (5). Although those for the EFT do not converge (infinite LECs), those components produced by the crossed-box diagram, V_{44} and V_{34}, in the covariant approach always converge. This also holds for the crossed-box part of the other components, V_{56} and V_{75}, but, in these cases, one has to consider a further contribution from the noncrossed box diagram. The convergence crucially depends on the way the iterated OPE is calculated but there is one choice, quite natural actually, that provides convergence as good as for the crossed-box diagram. Though it does not really make sense physically to integrate dispersion integrals over t' up to ∞, expressions so obtained provide a reliable benchmark, as far as the same physics is implied.

The second difference concerns the number of components. The covariant approach involves many more than the EFT one at NNLO (six instead of two). The extra ones imply some recoil effect and have a nonlocal character. They are of higher order in a $1/M$ expansion but, instead, in the large-t' limit, they compare to the others [see Eqs. (11)].

The third difference has to do with the large-M limit of the covariant approach, Eqs. (9), which allows one to recover the structure of the EFT results. The way this limit is taken in the H or G functions, or in the factor multiplying the first quantity, is quite rough. It assumes approximations like $x^2 + 4M^2q_\pi^2 \simeq 4M^2q_\pi^2$ $(2q_\pi M \geqslant x)$. Actually, owing to the small but finite value of the pion mass, there is a very little range of t' values $(t' - 4m_\pi^2 \leqslant m_\pi^4/M^2)$ where this approximation is not valid. The correction, which disappears in the chiral limit (zero pion mass), could affect the long-range part of the interaction.

The fourth difference involves chiral symmetry and related properties. Contrary to what is sometimes thought, fulfilling these properties in calculating the TPE contribution in the covariant approach is possible. This however supposes some elaboration, requiring that a description of the $N\bar{N} \to \pi\pi$ transition amplitude entering the dispersion relations is consistent with chiral symmetry. In the instance of the Paris model for the NN strong interaction [25], this amplitude could be related to experimental data. For the NN weak interaction, the strong amplitude was instead modeled from the contribution of a few nucleon resonances in the s channel [15]. This can be essentially achieved by adding the contribution of the $\Delta(1232\,\mathrm{MeV})$ resonance to the nucleon intermediate state retained here. This one, in the dispersion-relation formalism, suppresses the low-energy $N\pi \leftrightarrow N\pi$ strong-transition amplitude, otherwise dominated by a well-known large Z-type contribution inconsistent with chiral symmetry. This part, which involves two pions in an isosinglet state (with the σ-meson quantum numbers), is irrelevant here however. Its contribution is suppressed, in accordance with the Barton theorem [26], which states that the exchange of scalar and pseudo-scalar neutral mesons does not contribute to the PV NN interaction (assuming CP conservation). This feature largely explains why the PV TPE contribution has not been found as important as originally expected, on the basis of the strong-interaction case [15]. There is another part that is of interest here. It decreases the Z-type contribution [the first term of $V_{56}(q)$ in Eq. (15)] by an amount that corresponds to changing the factor g_A^3 into g_A in the first term of $V_{56}(q)$ in Eq. (20). This can be checked in the simplest nonrelativistic quark model according to the relation

$$g_{\pi NN}^2 - \frac{2g_{\pi N\Delta}^2}{9} = \left(1 - \frac{16}{25}\right) g_{\pi NN}^2 = \frac{9}{25} g_{\pi NN}^2 = \frac{g_{\pi NN}^2}{g_A^2}, \tag{21}$$

which shows that the contribution of nucleon resonances to the πN scattering amplitude can be accounted for by dividing the intermediate nucleon contribution by the factor g_A^2. A somewhat different but better argument is based on the Adler-Weisberger sum rule [27]. This one, which does not involve any nonrelativistic limit, can be cast into the form $1 - \int \cdots = 1/g_A^2$, where the integral involves the off-mass-shell pion-proton total cross sections. For simplicity, here we did not retain the Δ contribution, which is possibly improved for other resonances. We nevertheless keep in mind from the previous considerations that the discrepancy between the EFT and the covariant approaches, which was noticed for the contribution of the triangle diagram in the former one (a factor of g_A instead of g_A^3), could be removed by completing the latter one. The corresponding contribution, considered in Ref. [15], amounts to 10–20% of the one retained here.

A last remark concerns the comparison of the TPE with the ρ-meson exchange. The former was discarded in the past because of possible double counting with the latter one. In this respect, we notice that the ratio of the V_{44} and V_{34} components, which could contribute to PV effects in pp scattering ($^1S_0$–$^3P_0$ transition amplitude), is very much like the ratio of the local and nonlocal parts of a standard ρ-exchange contribution. There is some relationship between this result and the fact that the pion cloud produces a contribution to the anomalous magnetic moment of the nucleon, which compares to the physical one. The problem is different for the other PV transition, $^3S_1$–$^3P_1$, where the V_{56} component could contribute. The corresponding charged-ρ exchange of interest in this case is governed by the PV coupling $h_\rho'^1$, which was predicted to vanish in the DDH work [28]. A small value (-0.7×10^{-7}) was obtained by Holstein [29] by considering a pole model. A larger value $[-(2\text{–}3) \times 10^{-7}]$ was obtained later by Kaiser and Meissner [30] using a soliton model. In any case, these values lead to negligible effects. We however observe that the PV πNN coupling constant h_π^1 is also small in the same models, with most of its possible larger predicted value being due to the contribution of strange quarks [31]. Sizable values of $h_\rho'^1$ could thus be expected. On the basis of a dynamical model considering the ρ meson as a two-pion resonance, one cannot exclude values of $h_\rho'^1$ in the range of $(5\text{–}10)\sqrt{2}h_\pi^1$, a relation that the results of Kaiser and Meissner roughly verify. In contrast to the previous values, the last ones could lead to some double counting and it is likely that the $h_\rho'^1$ contribution to PV effects is then largely accounted for by the TPE considered in this work. It is conceivable that a similar conclusion holds for the other isovector coupling, h_ρ^1, which contributes to the PV effects in pp scattering as discussed earlier. Another aspect of the comparison with a ρ exchange concerns the range of

the TPE, which was presented in Ref. [6] as a medium one. This could apply to the exchange of two pions in a S wave (σ meson), which contributes to the strong NN interaction but is absent in the weak case, as already mentioned. The TPE of interest here involves two pions in a P wave with the quantum numbers of the ρ meson. Owing to a centrifugal barrier factor, the TPE contribution is shifted to values of t' higher than for a S wave, making the range of its contribution closer to a ρ-exchange one. Some numerical illustration is given in the next section.

V. NUMERICAL COMPARISON OF POTENTIALS

We consider in this section various numerical aspects of the potentials presented in the previous one. They successively concern the spectral functions, $g_{ij}(t')$, the potentials in momentum space, $v_{ij}(q)$, and the potentials in configuration space, $v_{ij}(r)$. In most cases, we directly compare the results of the covariant approach (COV) with those obtained from it in the large-M limit (LM) [Eqs. (20)]. This comparison is more meaningful than the one with the EFT potential (EFT) [Eqs. (12)] as it is not biased by the choice of the factor Λ_χ and by the difference of a factor g_A, instead of g_A^3, in part of the contribution to V_{56}, the origin of which is understood in any case. Before entering into details, we notice that the various components of the interaction have a local character for some of them (V_{44} and V_{56}) and a nonlocal one for the others (V_{34} and V_{75}). At low energy, however, it turns out that one of the contributions involving the factor $\vec{p}$ or $\vec{p}'$ in their expression, Eq. (7), is small. Moreover, with our conventions, the spin-isospin factors give the same values for the z component. The various components can then be usefully compared, independently of their local or nonlocal character, which is what we do here. In our numerical results we assume the following values: $g_{\pi NN} = 13.45$, $g_A = 1.2695$, $M = 938.919\,\text{MeV}$, $m_\pi = 138.039\,\text{MeV}$, and $m_\rho = 771.1\,\text{MeV}$.

We begin with the first four spectral functions $g_{ij}(t')$ entering potentials V_{44}, V_{34}, V_{56}, and V_{75}. Their t' dependence is shown for a range of $t'^{1/2}$ going from threshold to about 5 GeV in Fig. 4(a) to roughly evidence the relative weight of various components at small and high t'. At first sight, different potentials have comparable sizes. The small-t' range is physically more relevant in the sense that the regime beyond $1\,\text{GeV}^2$ is expected to involve the contribution of other multimeson exchanges. The higher t' range is more appropriate to illustrate convergence properties. At low values of t', one can see some significant differences as expected from the $1/M$ expansion, Eq. (18). For $t'^{1/2} \leqslant 0.5\,\text{GeV}$, the spectral functions entering the local potentials V_{44} and V_{56} dominate those of the nonlocal ones, V_{34} and V_{75}. All of them increase in the lower t' range (except in a very small t' range for V_{56}) and one has to go to much higher values of this variable to observe some saturation and ultimately some decrease. The maximum is roughly reached around $t'^{1/2} = 2M$, which, apart from the pion mass, is the only quantity entering the calculations. The decrease, roughly given by $t'^{-1/2}$, up to log terms, ensures good convergence properties for potentials $v_{ij}(q)$, Eq. (5) (which would not be the case for the other Green function mentioned in the text; see details in Appendix A2). The validity of the $1/M$ expansion for the spectral functions $g_{44}(t')$ and $g_{56}(t')$, which allows one to recover the EFT results for the essential part, can be checked by examining Fig. 4(b), where the "covariant" and approximate results are shown for a t' range extending to $1\,\text{GeV}^2$. It is observed that the dominant term in the $1/M$ expansion tends to overestimate the more complete results both at very low and high values of t'. In the first case, the threshold behavior [q_π^3 for $g_{44}(t')$ and $\arctan(m_\pi^2/q_\pi M)$ for $g_{56}(t')$] is missed (see the observation on the $1/M$ expansion in the previous section). In the second case, the overestimation, which is roughly given by a factor of t'/M^2, tends to increase with t', preventing one from getting convergent results.

In Fig. 5(a), we show the potentials $v_{ij}(q)$ up to $q = 1$ GeV (together with the OPE one, which has a strong dependence on q and is divided by 10 to fit the figure). As expected from examination of the spectral functions, the TPE potentials have roughly the same size and there is no strong evidence that some of them should be more important than others. It is also noticed that their decrease in the range $q = 0$–1 GeV is slower than the standard ρ-exchange one, given by $1/(m_\rho^2 + q^2)$, indicating they roughly correspond to a shorter range interaction. The comparison of the potentials $v_{44}(q)$ and $v_{56}(q)$ with the corresponding EFT ones, Eqs. (12), can be made by looking at Fig. 5(b). The choice of Λ_χ in the EFT results ($\Lambda_\chi = 4\pi g_A M/g_{\pi NN}$) is suggested by the large-M limit of the "covariant" expression [see Eqs. (20)] to make the comparison as meaningful as possible. A striking feature appears here: The EFT potentials have a sign opposite to the "covariant" ones but

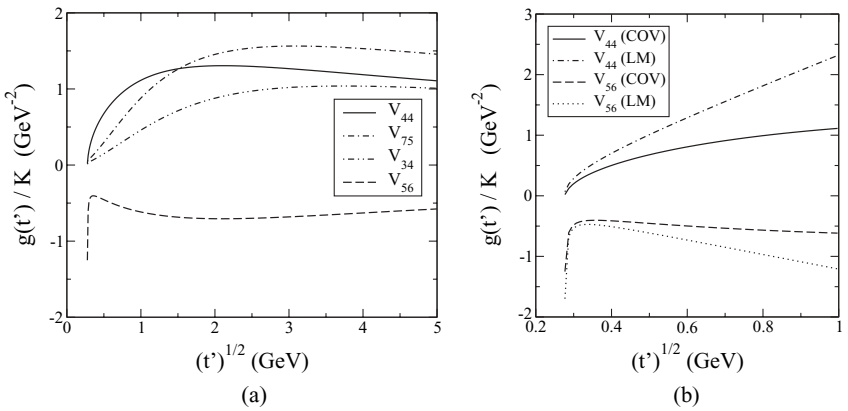

FIG. 4. Spectral functions $g(t')$ in units of GeV^{-2}, with the coefficient $\tilde{K}$ factored out, and represented as a function of $t'^{1/2}$ to better emphasize the low-t' range, for (a) $t'^{1/2}$ from threshold to 5 GeV for all functions, to show the relative importance of the various components and the beginning of the onset of the asymptotic behavior, $t'^{-1/2}$ and (b) from threshold to 1 GeV for functions $g_{44}(t')$ and $g_{56}(t')$ together with their large-M limits, to check the validity of this approximation.

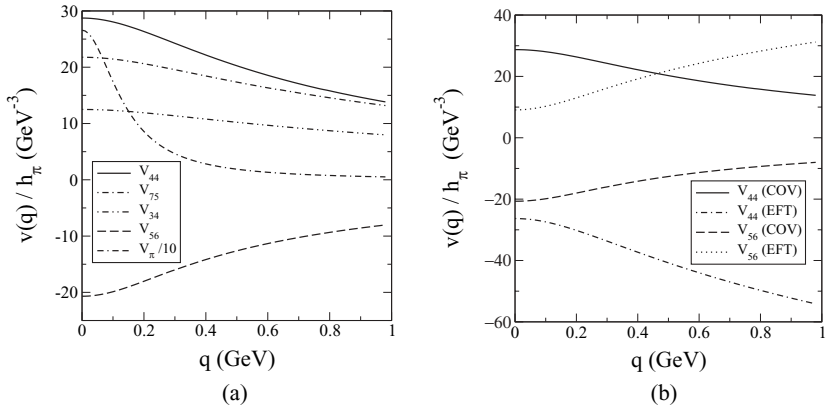

FIG. 5. Potentials $v_{44}(q)$, $v_{34}(q)$, $v_{56}(q)$, and $v_{75}(q)$ (together with the OPE one divided by 10) for q ranging from 0 to 1 GeV (a) and their EFT counterpart for $v_{44}(q)$ and $v_{56}(q)$ (b). Ingredients entering the EFT results are specified in the text. Notice that the EFT and "covariant" versions of a given component of the potential have opposite signs.

the q dependence is roughly the same. This feature suggests that the LEC part could play an important role.

To make a more significant comparison, we subtracted a constant from both potentials so that they vanish at $q^2 = 0$. This procedure amounts to using subtracted dispersion relations, which leads to convergence in all cases. Moreover, in configuration space, this part of the interaction determines the long-range component of the potential, which is physically the most relevant one. Results are shown in Fig. 6. The "covariant" and LM results now have the same sign. It is however noticed that the present LM results tend to overestimate the "covariant" ones. In the limit $q \to 0$, the overestimate reaches a factor 1.6 for V_{44} and a factor 1.3 for V_{56}. This points in this case to the role of higher $1/M$-order corrections. Actually, the discrepancy vanishes in the limit $m_\pi/M \to 0$, showing that the nonzero pion mass has some effect. The discrepancy tends to slowly increase with q (by factors of 1.9 and 1.5 at $q = 1$ GeV for V_{44} and V_{56}, respectively), pointing to the role of $\ln(q)$ corrections appearing in the large-M limit. Altogether, these results are in accordance with the overestimate already noticed for spectral functions in this approximation. From a different viewpoint, these results confirm the expectation that the discrepancy between the EFT and "covariant" approaches

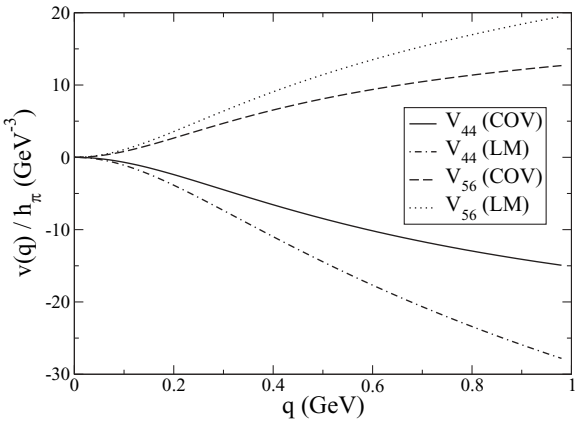

FIG. 6. Subtracted potentials $v_{44}(q)$ and $v_{56}(q)$ for q ranging from 0 to 1 GeV, comparing the large-M limit approach [LM, Eqs. (20)] with the covariant one. The asymptotic q dependence of the "covariant" results is a constant one whereas the one for large-M limit results has an extra $\ln(q)$ dependence.

shown in Fig. 5(b) can be ascribed to contact terms. A rough agreement would be obtained with the effective potential obtained in the $\overline{\text{MS}}$ together with a dimensional-regularization scale μ ranging from $3m_\pi$ to $6m_\pi$, depending on how this is made (see the definition of this scheme at the end of Appendix B).

The Fourier transforms of the $v_{ij}(q)$ quantities, $v_{ij}(r)$, are shown in Fig. 7(a) for small distances and in Fig. 7(b) for intermediate distances. We call them potentials though they are dimensionless quantities, the energy dimension being given by the extra operators $\vec{p}$. They are multiplied by a factor r^2 to emphasize the range that is relevant in practice for calculations. At small distances, the comparison of various components roughly reflects the one for spectral functions or potentials in momentum space. Examination of these results at large distances evidences some significant differences. They have a better agreement with expectations from the $1/M$ expansion or from the very low t' behavior of spectral functions. Thus, the local potentials, $v_{44}(r)$ and $v_{56}(r)$, have a range larger than the other two components, $v_{34}(r)$ and $v_{75}(r)$, do. The differences appear only in the range where potentials have small contributions to PV effects.

The comparison with the LM potentials is given in Fig. 8 for the local components (V_{44} and V_{56}). It is noticed that these last potentials should be completed by contact terms, which have a sign opposite to the corresponding curves. Because of the difficulty of representing these terms in a simple way, they have not been drawn in this figure. Moreover, they are not distinguishable from the LEC contributions and thus have an arbitrary character (i.e., they depend on the subtraction scheme). Considering first potentials at intermediate (or long) distances, where they can be the most reliably determined, one finds that the LM and "covariant" potentials have the same sign despite their having opposite sign in momentum space. This result is in complete accordance with the subtracted potentials shown in Fig. 6. Indeed, the slope of the corresponding results is, up to a minus sign, a direct measure of the square radius of the potential weighted by its strength. The negative slope for the potential V_{44} thus indicates that its configuration-space representation is positive at intermediate distances (the opposite for V_{56}). Quantitatively, the significant dominance of the LM results over the "covariant" ones (by factors of 1.7 and 1.4 for V_{44} and V_{56}, respectively, at $r = 0.8$ fm) confirms what is found for subtracted potentials in momentum space.

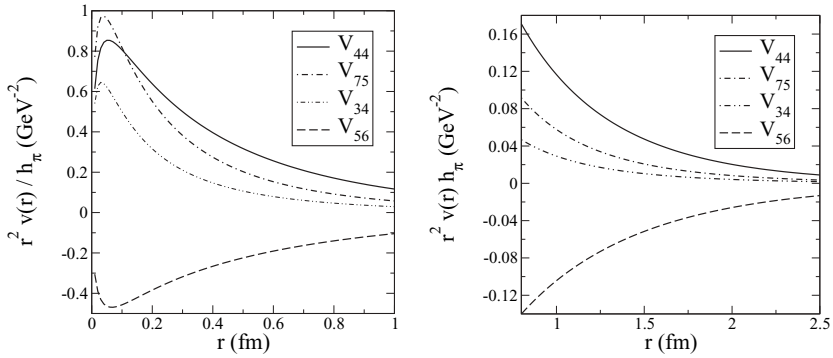

FIG. 7. Potentials $v_{44}(r)$, $v_{34}(r)$, $v_{56}(r)$, and $v_{75}(r)$ at (a) small and (b) intermediate distances. The results shown in the figure represent these potentials multiplied by a phase factor of r^2 (in units of GeV^{-2}) to better emphasize the most relevant range for applications.

Considering now the very short range domain, one finds that the product of the LM potentials with r^2, which are shown in Fig. 8(a), diverge like $1/r$ when $r \to 0$, up to log factors. The contribution of this part alone to the plane-wave Born amplitude is thus logarithmically divergent. This contribution turns out to be canceled by the zero-range one, mentioned previously, so that the sum is finite. Thus, there is no principle difficulty with this peculiar behavior of the LM potentials in configuration space but, of course, some care is required in estimating their contribution.

Naively, it could be thought that the TPE is a medium-range interaction, as already mentioned. In Fig. 9, we compare potentials $v_{44}(r)$ and $v_{56}(r)$ to a standard rho-exchange one normalized so that they have the same volume integral. This quantity determines the low-energy plane-wave Born amplitude (up to a factor of $\vec{p}$, which can be factored out). At very large distances, the effect of the longer-range TPE tail is evident but this occurs in a domain where the potential is quite small and will not contribute much. At intermediate or even at small distances, however, the TPE roughly compares to the ρ exchange. Actually, it turns out to have a shorter range. This reflects the fact that the two-pion continuum has an unlimited mass (with the integration over t' extending to infinity). Moreover, it is slightly more singular at very small distances, as a result of the extra $\ln(r)$ dependence of the TPE potential. This last effect is typical of relativistic effects. Both long- and short-distance effects can be traced back to the $g(t')$ function, which, in the TPE case, extends to both small and large values of t' with a maximum around $t' = 4M^2$, whereas it is concentrated around $t' = m_\rho^2$ for the ρ-exchange one [a $\delta(t' - m_\rho^2)$ function in the zero-width limit].

For simplicity, we did not consider explicitly the contribution from nucleon resonances in the two-pion box diagrams, which was accounted for in the 1970s in a "covariant" approach [15] or recently in an EFT [16,17] or a TO one [18]. As already mentioned, part of it is contained in the EFT approach by relying on the Weinberg-Tomozawa description of the πN scattering amplitude. It only contributes to the V_{56} component and could represent 10–20% of the total contribution, depending on the range and how it is estimated. On top of it, there are further contributions that affect both V_{44} and V_{56} components. In the case of V_{44}, they amount to an extra 30–40% contribution around 1 fm in the "covariant" calculation [15] and roughly twice as much in the EFT approach [16,17] or the TO one [18]. For the case of V_{56}, it is more complicated, as the aforementioned contribution relative to the description of the πN scattering amplitude has to be disentangled first for the "covariant" calculation. When this is done, the extra contribution from resonances decreases and could represent 30–40% of the contribution with nucleons only [15]. This is slightly less than what is obtained in the EFT approach [16]. By taking into account that the EFT results overestimate the "covariant" ones for the nucleon intermediate state, it thus appears that the overestimate for the resonance intermediate state is significantly larger. This feature points to corrections of order $p^2/[M(M_\Delta - M)]$ affecting the resonance propagator (dispersion effects), which are known to be important, whereas corrections in relation with the large-M

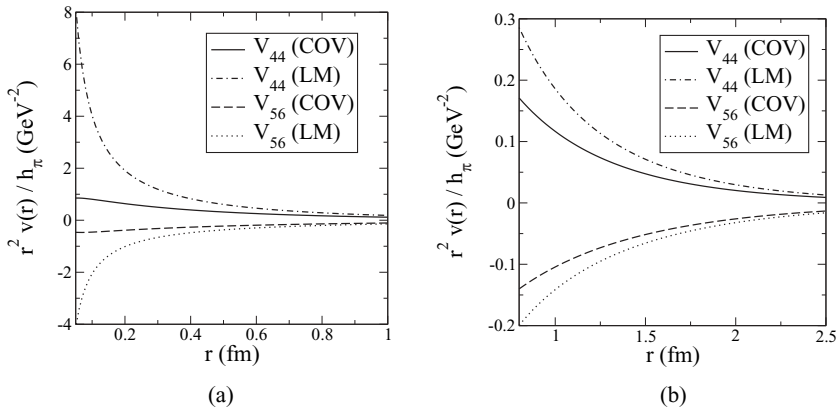

FIG. 8. Potentials $v_{44}(r)$ and $v_{56}(r)$ at (a) small and (b) intermediate distances, comparing the "covariant" calculations with their large-M limits; other definitions or comments are as in Fig. 7. The curves corresponding to the large-M limit in (a) tend to ∞ when $r \to 0$ and have a zero-range part (not shown in the figure) with an opposite sign.

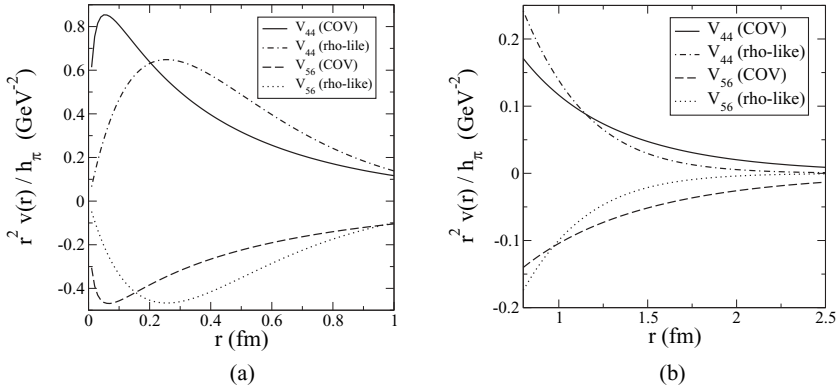

FIG. 9. Potentials $v_{44}(r)$ and $v_{56}(r)$ at (a) small and (b) intermediate distances, comparing the "covariant" calculations with a standard rho-exchange potential normalized to the same volume integral; other definitions or comments are as in Fig. 7.

limit are of order p^2/M^2. This reinforces the conclusion of Ref. [16] that, in contrast to the strong-interaction case, the role of resonances, especially the $\Delta(1232\,\mathrm{MeV})$ one, plays a negligible role in the PV NN interaction.

VI. ESTIMATES OF PV EFFECTS IN TWO PROCESSES

The TPE potentials considered here have an isovector character. At low energy, they can contribute to two different transitions, ${}^1S_0$–${}^3P_0$, which involves identical particles such as two protons or two neutrons, and ${}^3S_1$–${}^3P_1$, which involves different particles. The interactions V_{44} and V_{34} contribute in the first case while the interactions V_{56} and V_{75} contribute in the other. Two processes of current interest where the TPE potentials matter, are, respectively, proton-proton scattering and radiative neutron-proton capture at thermal energy. In the first case, a helicity dependence of the cross section, $A_L(E)$, has been measured at different energies [32–34]. In the second case, an asymmetry in the direction of the photon emission with respect to the neutron polarization, A_γ, has been looked for at LANSCE [35] (and the experiment is now running at SNS). The TPE contribution to these effects is discussed in the following. The calculations have been performed with the NN-strong-interaction model, Av18 [36], which is local wave by wave. Vertex form factors are ignored. On the one hand, the dispersion-relation formalism assumes on-mass-shell particles, with the contribution from form factors in other approaches being generated by what is included in the dispersion relations. On the other hand, the role of form factors was already examined within the EFT approach [10,11], partly with the motivation of regularizing a potential that is badly behaved at short distances, $\propto [r^{-3} - c\delta(\vec{r})]$, where c is infinite and "determined" so that the integral over $\vec{r}$ has a well-defined value. There is no principle difficulty to work with this potential, however,[4] and we will therefore use it here. This will facilitate the comparison with the "covariant" results.

As a side remark, we notice that form factors different from those mentioned here have been used in the context of applying effective field theories to the strong NN interaction [4]. They involve a separable dependence of the relative momentum in the initial and final states, $\vec{p}$ and $\vec{p}'$, instead of $\vec{q} = \vec{p} - \vec{p}'$. Their effect is to smooth out wave functions at short distances in accordance with the idea that the corresponding physics, partly unknown, should be integrated out and accounted for by LECs. For such form factors, it would be more convenient to work in momentum space. However, in the case where configuration space is chosen, the methods we used for dealing with the badly behaved potential could be useful there too.

A. Proton-proton scattering

The first calculation of TPE effects was done by Simonius [37], with the aim of estimating a measurement of PV effects in pp scattering (since the Cabibbo model then used was not contributing to the pp force in its simplest form). Our results, obtained here for three energies at which the longitudinal asymmetry $A_L(E)$ has been measured, are presented in Table I.

Examining the "covariant" results, one finds that the contribution of the local term, V_{44}(COV), dominates over the nonlocal one, V_{34}(COV), which appears at the next order in the $1/M$ expansion. The result could be guessed from looking at Fig. 7. Their ratio is of the order of the factor $1 + \mu_V = 4.706$, which appears in the ρ-exchange potential. There are reasons to think this result is not accidental (see the end of Sec. IV). The present results compare to the earlier ones [37] as well as with the value $A_L(13.6\,\mathrm{MeV}) = -0.1h_\pi^1$, which has been used in analyses of PV effects [31]. The closeness can be attributed to the fact that the Av18 model employed here and the Reid or Hamada-Johnston models previously used are local ones and, moreover, evidence a strong short-range repulsion. Significant departures could occur, instead, with models such as CD-Bonn [38] or some Nijmegen ones [39], which have

TABLE I. PV asymmetries in pp scattering at three energies (13.6, 45, and 221 MeV), successively for the potentials V_{44}(COV), V_{34}(COV), V_{44}(rho-like), and V_{44}(LM), in units of the h_π^1 coupling constant.

Energy (MeV)	13.6	45	221
V_{44}(COV)	−0.092	−0.154	0.072
V_{34}(COV)	−0.022	−0.042	−0.029
V_{44}(rho-like)	−0.110	−0.196	0.096
V_{44}(LM)	−0.150	−0.252	0.127

[4]The trick is to separate in the integrands a part determined by wave functions at the origin, of which the integral over $\vec{r}$ is known, from the remaining part, which is well behaved at the origin.

a nonlocal character (see Ref. [40] for a discussion about the role of nonlocality).

Because of its long-range component, one could infer that the TPE contribution should be enhanced with respect to the ρ-exchange one when the effect of short-range repulsion is taken into account. The comparison of V_{44}(rho-like) and V_{44}(COV) results shows that this is the other way round. This can be explained by the fact that the long-range contribution where the TPE dominates over the ρ-exchange has little contribution to the asymmetry (a few percent). Instead, the short-range contribution where the TPE dominates over the ρ-exchange plays a bigger role. The effect of short-range repulsion on this contribution will therefore be enhanced, hence decreasing the total TPE contribution with respect to the ρ-exchange one.

B. Asymmetry in neutron-proton radiative capture

In contrast to pp scattering, the asymmetry A_γ involves a nonzero contribution from OPE. Thus, independently of the value of the coupling h^1_π, one can directly compare the TPE and OPE contributions. The last one has been extensively studied (see Ref. [41] and earlier references therein and Refs. [10,11, 42] for more recent works). Its contribution is approximately given by $A_\gamma(\text{OPE}) = -0.11h^1_\pi$ ($= -0.112h^1_\pi$ for the Av18 model used here).

The TPE contributions to A_γ for the "covariant" case are given by

$$\begin{aligned} A_\gamma[V_{56}(\text{COV})] &= 0.0093h^1_\pi, \\ A_\gamma[V_{75}(\text{COV})] &= -0.0040h^1_\pi, \end{aligned} \tag{22}$$

and those for the rho-like and large-M limit are

$$A_\gamma[V_{56}(\text{rho-like})] = 0.0093h^1_\pi, \tag{23}$$

$$A_\gamma[V_{56}(\text{LM})] = 0.0141h^1_\pi. \tag{24}$$

Considering the "covariant" results, one first notices that the contribution of the local term, V_{56}(COV), dominates over the nonlocal one, V_{75}(COV), which appears at the next $1/M$ order. The effect is however less important than in pp scattering, which can be inferred from looking at the corresponding potentials in Fig. 7. Moreover, in contrast to this process, their contributions have opposite signs. Thus, the total contribution represents only -5% of the OPE one. This is good news in the sense that it confirms that the asymmetry A_γ represents the best observable to determine the coupling h^1_π. The present results reasonably compare to an earlier one [19]: $A_\gamma(\text{TPE}) = 0.008h^1_\pi$, which comes from adding up $A_\gamma(V_{56}) = 0.0107h^1_\pi$ and $A_\gamma(V_{75}) = -0.0027h^1_\pi$. Part of the difference for $A_\gamma(V_{56})$ can be traced back to the omission here of the Δ resonance contribution in intermediate states. Recall that this contribution tends to make the πN-scattering amplitude consistent with the Weinberg-Tomozawa coupling, resulting in an enhancement of the V_{56} interaction (see the discussion in Sec. IV). The main difference for $A_\gamma(V_{75})$ is due to the extension of the integration over t' in the dispersion relation from $50m^2_\pi$ to ∞ here.

At first sight, the comparison of the TPE and ρ-exchange results, which are essentially the same, shows features different from those observed in pp scattering. Examination of Fig. 9 indicates that, in comparison to the V_{44} potential, the enhancement of the TPE potential, V_{56}(COV), over the ρ-exchange one, V_{56}(rho-like), is larger at large distances and smaller at short distances. As a result, the two effects from the short-range repulsion mentioned for pp scattering tend to cancel here.

C. Results in the large-M limit

For the subtraction of an infinite term, results obtained in the large-M limit, which can be identified with the EFT ones for the essential part, cannot be directly compared to the "covariant" ones. A first look nevertheless shows that the results, apart from an enhancement by a factor of 1.5 or so, are very similar. Moreover, from considering the plane-wave Born approximation, we should have expected opposite signs. It is therefore appropriate to give some explanation to help understand these results.

We first checked which range was contributing to PV asymmetries and found that the role of the range below 0.4–0.5 fm was rather small (10–20%). The observed enhancement of the large-M result over the "covariant" one thus reflects the similar enhancement that can be inferred from the corresponding potentials in Fig. 8, around 0.8 fm. The small role of the range below 0.4–0.5 fm is not expected from considering Fig. 7. Instead, it can be related to the strong interaction model, Av18, used to calculate wave functions entering estimates of observables. This model evidences the effect of a strong repulsion at short distances. As this effect is much less pronounced with nonlocal models, one can expect that the use of models such as CD-Bonn or some Nijmegen ones will show some differences with the present results. We can anticipate an increase of the magnitude of the "covariant" results and a decrease of the LM ones (without excluding in this case a change in sign for the plane-wave Born approximation).

While trying to understand the role of higher $1/M$-order corrections, we face the problem that the corresponding contributions to potentials are more singular than those for V_{44}(LM) or V_{56}(LM), requiring some regularization and introduction of further LECs. Restricting our study to the range $r \geqslant 0.4$–0.5 fm, which provides most of the contribution to the PV asymmetries, we found that the contribution at the next $1/M$ order had a sign opposite to the dominant one, which it largely cancels in the range around 0.8 fm. The correction, which is larger than needed, suggests that other corrections are necessary to ensure reasonable convergence. Among them, one could involve chiral symmetry breaking. We checked that in the limit of a massless pion, the "covariant" potential $v_{44}(r)$ and its large-M limit are significantly closer to each other. A nonzero pion mass could thus explain a sizable part of the discrepancy for observables between the "covariant" and the large-M-limit results. We notice that the comparison of the EFT and "covariant"approaches in the strong interaction case evidences features similar to those here (see Ref. [21] and references therein). As far as we can see, the similarity is only partial.

The large-M limit of "covariant" potentials assumes a particular subtraction scheme. In another scheme, the $\overline{\text{MS}}$

one, part of the functions $L(q)$ appearing in Eqs. (20), are replaced by $L(q) - 1 - \ln(\mu/m_\pi)$ (see Appendix B). Because of the effect of short-range repulsion in the Av18 model, the correction has little effect on the calculated observables (an increase of a few percent for the S–P transition part). This would be different for nonlocal models where the correction could be significantly larger. Depending on the value of the parameter μ, a large part of the sensitivity of the LM results to strong-interaction models mentioned here could be removed [10]. We notice that a discussion similar to the one here on the role of the subtraction scheme has also been held in the strong-interaction case [4]. It was concluded that the spectral function regularization (SFR) scheme was providing better convergence properties than the dimensional-regularization one, owing to its avoidance of spurious short-range contributions. To some extent, the SFR scheme is close to the $\overline{\text{MS}}$ one considered here, with the parameter $\tilde{\Lambda}$ introduced in the former case being replaced by the quantity 2μ in the latter case.

VII. CONCLUSION

In the present work, we have compared different approaches for incorporating the TPE contribution to the PV NN interaction. They include a covariant one, which fully converges and can thus be considered as a benchmark, and an effective-field-theory and a time-ordered one, which can contain infinities. The last two approaches involve two components at the leading order, with a local character, whereas the covariant one involves both local and nonlocal components. For a given transition, one can thus compare the local components obtained from different approaches with local components on the one hand and the nonlocal ones on the other hand. These two comparisons can allow one to assess the validity of the assumption of dominant order in the EFT approaches as well as the role ascribed to LECs.

We first notice that the EFT approach, the time-ordered-diagram approach, and the limit of the covariant one at the lowest nonzero order in the $1/M$ expansion essentially agree with each other for the local terms. Possible discrepancies involve ingredients that have been omitted (the contribution of baryon resonances in particular) but these are unimportant for the comparison. We can thus concentrate on a comparison of the covariant approach with its LM limit. Taking into account that this approach is determined up to contact terms, one finds rough agreement. This is better seen by considering the subtracted potentials in momentum space or intermediate distances ($r = 1$ fm) in configuration space. Quantitatively, the LM (EFT) approach tends to overestimate the "covariant" results. At low q or at intermediate distances, the effect reaches factors of 1.7 and 1.3, respectively, for the transitions ${}^1S_0$–${}^3P_0$ and ${}^3S_1$–${}^3P_1$. At very small but finite distances, the LM (EFT) potentials become very singular and their contribution to physical processes diverge. This divergence is canceled by the contribution associated with the contact term so that the total result is finite (after renormalization). This peculiar behavior at and around $r = 0$ contrasts with the smooth but diverging behavior in momentum space of the published EFT TPE interaction. In this case, it turns out that the sign of the potential is opposite to that one at finite distances, which is the most relevant part. This suggests that this EFT TPE potential is dominated by an unknown contact term, as far as a comparison with the "covariant" result is concerned. The problem disappears with a different subtraction scheme, such as the minimal one with a dimensional-regularization scale μ in the range $(3–6)m_\pi$. This last choice tends to minimize the role of short distances, confirming the absence of a large sensitivity to cutoffs observed elsewhere [10]. Interestingly, the $\overline{\text{MS}}$ scheme corresponds to cutting off the dispersion integrals at a value of $t'^{1/2}$ around 2μ, which, together with the aforementioned value of μ, is about 1–2 GeV. This is quite a reasonable value for separating the contribution of known physics from the unknown part to be integrated out. We thus believe that the choice of the $\overline{\text{MS}}$ scheme would be more appropriate; the interaction then ascribed to the EFT TPE one, would be a better representation of the most reliable part of the TPE physics, which occurs at intermediate and large distances.

Comparing the nonlocal components to the local ones, one finds that they are rather suppressed at large distances. For such distances, the contribution to dispersion relations is expected to come from values of t' smaller than M^2. The suppression of nonlocal terms then reflects the fact that they have an extra $1/M$ factor in the $1/M$ expansion. At short distances, instead, the contribution to dispersion relations comes from large values of t'. In this case, the local and nonlocal terms have the same $1/M$ order and they tend to have comparable contributions. Another aspect of the dependence on the range concerns the comparison with the ρ-meson exchange. Not surprisingly, TPE dominates the ρ-meson exchange at long distances but, because the potential is relatively small there, not much effect is expected from this part on the calculation of observables. The TPE contribution is slightly dominated by the ρ-meson exchange one at medium distances and dominates again at very short distances. Taking into account that the dominant contributions come from short and intermediate distances, one finds that the TPE contribution has a shorter range than the ρ-meson exchange.

We looked at the TPE contribution in two physical processes, pp scattering and radiative thermal neutron-proton capture. Roughly, they confirm what could be inferred from examining potentials. The results from the "covariant" approach, calculated with the Av18 NN strong-interaction model, essentially agree with earlier estimates based on other models. The main discrepancies highlight the role of inputs such as the restriction on the t' value in the dispersion relations or the role of resonances in modeling the πN scattering amplitude that enter these relations but were omitted here for simplicity. Despite that plane-wave Born amplitudes calculated with the EFT TPE and those from the "covariant" approaches have opposite signs, it turns out that their contributions to observables are relatively close to each other. This feature points to the Av18 model, which produces wave functions that evidence the effect of a strong repulsion at short distances. Such a property is interesting in that the main contribution to observables comes from intermediate and long distances, where the derivation of the TPE potential is the most reliable. It is thus found that the EFT TPE at NNLO tends to overestimate the "covariant" results by about 50%, pointing

to a non-negligible role of next-order corrections. This is confirmed by the consideration of nonlocal terms, which correspond to higher order terms. Their contribution is especially important in neutron-proton capture, owing to a destructive interference with the dominant one. Thus, the result at the dominant $1/M$ order (LM) in this process exceeds the "covariant" one by a factor of about 2–3. Interestingly, the present results are rather insensitive to the subtraction scheme since the coefficient $1 + \ln(\mu/m_\pi)$ remains in the range of a few units. This is a consequence of the strong short-range repulsion present in the Av18 model. We however stress the fortunate character of this result. The use of nonlocal strong-interaction models, such as CD-Bonn or some Nijmegen ones, could lead to different conclusions. Actually, the dependencies on the model expected for the contribution of the term $1 + \ln(\mu/m_\pi)$ and the EFT potential calculated in the MX scheme are likely to largely cancel.

By comparing different approaches to the description of the PV TPE NN interaction, it was expected that one could learn about their respective relevance. By implying a natural cutoff of the order of the nucleon mass, the "covariant" approach provides an unavoidable benchmark. This is of interest for the EFT approach, which, up to now, has been considered at the lowest $1/M$ order. In improving this approach, a first step concerns the subtraction scheme. The minimal-subtraction one ($\overline{\text{MS}}$), which involves a renormalization scale μ, is probably more favorable. By taking for this scale a value of the order of the nucleon mass (or the chiral-symmetry-breaking scale Λ_χ), the scheme better matches the separation of the interaction into known and less-known contributions, corresponding, respectively, to long and short distances. The LECs so obtained could be less dependent on the strong-interaction model. The next step should concern higher $1/M$-order terms, whose contributions are not negligible. This is likely to require a lot of cautious work, as the singular behavior of these terms at short distances increases with their order. Meanwhile, the "covariant" results could provide both a useful estimate and a relevant guide for their study.

ACKNOWLEDGMENTS

We thank the Institute for Nuclear Theory at the University of Washington for its hospitality and the Department of Energy for partial support during the completion of this work. We are grateful to Prof. U. van Kolck for pointing out an inconsistency of the simplest time-ordered-diagram approach with chiral-symmetry expectations. The work of CHH was supported by the Korea Research Foundation Grant funded by the Korean Government (MOEHRD, Basic Research Promotion Fund) (KRF-2007-313-C00178). The work of SA was supported by the Korea Research Foundation and the Korean Federation of Science and Technology funded by the Korean Government (MOEHRD, Basic Research Promotion Fund) and SFTC Grant No. PP/F000488/1. The work of CPL was supported in part by the U.S. Department of Energy under Contract No. DE-AC52-06NA25396.

APPENDIX A: SUBTRACTION OF THE ITERATED OPE AND RELATED QUESTIONS

A. Expressions of the spectral functions, $g(t')$

Historically, the derivation of the isovector PV TPE started with the calculation of the crossed diagram [12]. The calculation of the noncrossed diagram, which implies the removal of the iterated OPE contribution and thus requires more care, came slightly later [13].[5] Later works along the same lines [14,15] considered the two types of diagrams on the same footing. We first recall here some results relative to the crossed and noncrossed diagrams with the notation of Ref. [13] (functions $g_A(t')$, $g_B(t')$, $g_C(t')$, $g_D(t')$, and $g_E(t')$, respectively). The functions $g_A(t')$ and $g_D(t')$ correspond to the same spin-isospin structure. The two versions of the iterated OPE discussed in the text, which concern the $g_D(t')$ and $g_E(t')$ functions, are considered. The one employed in Ref. [13] corresponds to the term with the factor $(E + M)$ in the integrand whereas the other one considered in later works contains the factor $2E$. The expressions read

$$
\begin{aligned}
g_A(t') &= \frac{1}{2M}\left(\frac{G}{x} - \frac{Hx}{x^2 + 4M^2 q_\pi^2}\right),\\
g_B(t') &= \frac{x}{M^2} g_A(t'),\\
g_C(t') &= \frac{1}{2M}\left[\frac{4q_\pi}{\chi^2} + \frac{H}{M^2} - G\left(\frac{1}{M^2} + \frac{1}{\chi^2}\right)\right],\\
g_D(t') &= -\frac{x}{M^2 m_\pi^2}\arctan\left(\frac{m_\pi^2}{2Mq_\pi}\right) - \frac{G}{2xM}\\
&\quad + \int_{k_-^2}^{k_+^2} \frac{dk^2}{k^2\sqrt{k^2 t' - \left(m_\pi^2 + k^2\right)^2}}\\
&\quad \times \left[\frac{2E\text{or}(E+M)}{E^2}\left(\frac{k^2 - x}{4M} - \frac{E - M}{2}\right) + \frac{x}{2M^2}\right],\\
g_E(t') &= \frac{4x^2}{M^2 m_\pi^2 t'}\arctan\left(\frac{m_\pi^2}{2Mq_\pi}\right) + \frac{2G}{Mt'}\\
&\quad + \int_{k_-^2}^{k_+^2} \frac{dk^2}{k^2\sqrt{k^2 t' - \left(m_\pi^2 + k^2\right)^2}}\\
&\quad \times \left[\frac{2E\,\text{or}\,(E+M)}{E^2}\left(\frac{(k^2 - x)^2}{Mt'}\right.\right.\\
&\quad \left.\left. - \frac{2(E - M)(k^2 - x)}{t'} + \frac{(E - M)^2}{M}\right) - \frac{2x^2}{M^2 t'}\right],
\end{aligned}
\tag{A1}
$$

where the various functions q_π, x, χ, G, and H are given in the text [Eq. (10)]. The writing slightly differs from that in Ref. [13]. No nonrelativistic approximation is made for the integrands. Moreover, the original term, $\arctan(2Mq_\pi/m_\pi^2)/m_\pi^2$, has been transformed into $[\pi/2 - \arctan(m_\pi^2/2Mq_\pi)]/m_\pi^2$ and the factor $\pi/2/m_\pi^2$ has been inserted in the integral using the

[5] However, the paper contains errors that could obscure its understanding: The contents of Figs. 1 and 2 should be interchanged and the number -1.61 in the table should be replaced by -0.61.

relation $\int_{k_-^2}^{k_+^2} dk^2/(k^2\sqrt{k^2t'-(m_\pi^2+k^2)^2}) = \pi/m_\pi^2$. With this rearrangement, it can be checked that the integrand has no singularity at $k^2 = 0$.

The $g(t')$ functions considered in the present work are related to these by the relations

$$\begin{aligned} g_{44}(t') &= \tilde{K}\, g_C(t'), \\ g_{34}(t') &= \tilde{K}\, g_B(t'), \\ g_{56}(t') &= \tilde{K}[g_A(t') + g_D(t')], \\ g_{75}(t') &= \tilde{K}\, g_E(t'), \end{aligned} \tag{A2}$$

where $\tilde{K}$ is an overall constant given in Eq. (10). An important point to note is that the contributions of the term $G/2xM$ in $g_A(t')$ and $g_D(t')$, which dominate at low energy, exactly cancel. This cancellation is important in restoring the crossing symmetry for pions, a property that is fulfilled by the effective pion-nucleon interaction introduced in the EFT approach (triangle diagram).

B. Asymptotic behavior of the $g(t')$ functions

The asymptotic behavior of the spectral functions $g_{44}(t')$ and $g_{34}(t')$, which only involve the crossed-diagram contribution, can be easily obtained from their expressions, Eqs. (9). The dominant term is of the order $1/(M\sqrt{t'})$ up to some log factors [see Eq. (11)]. The asymptotic behavior of the two other spectral functions, $g_{56}(t')$ and $g_{75}(t')$, is considerably more complicated. Their analytic part contains terms with the behavior $-\tilde{K}\sqrt{t'}/2M^3$ and $\tilde{K}\sqrt{t'}/M^3$, respectively, whereas the integral part requires careful examination.

The dominant term in the integral is given by the part proportional to x and x^2 in the integrands of $g_{56}(t')$ and $g_{75}(t')$, respectively. As the integrands are the same up to a factor of $-4x/t'$, it is sufficient to consider the first case. Its contribution becomes

$$\begin{aligned} I_{56} &= -\tilde{K}x \int_{k_-^2}^{k_+^2} \frac{dk^2}{k^2\sqrt{k^2t' - \left(m_\pi^2+k^2\right)^2}} \\ &\quad \times \left(\frac{2E(\text{or}E+M)}{4ME^2} - \frac{1}{2M^2}\right) \\ &= \tilde{K}x \int_{k_-^2}^{k_+^2} \frac{dk^2}{k^2\sqrt{k^2t' - \left(m_\pi^2+k^2\right)^2}} \\ &\quad \times \left[\frac{(E-M)}{2M^2E}\left(\text{or}\frac{(E-M)(2E+M)}{4M^2E^2}\right)\right] \\ &= \tilde{K}x \int_{k_-^2}^{k_+^2} \frac{dk^2}{\sqrt{k^2t' - \left(m_\pi^2+k^2\right)^2}} \\ &\quad \times \left[\frac{1}{2M^2E(E+M)}\left(\text{or}\frac{(2E+M)}{4M^2E^2(E+M)}\right)\right], \end{aligned} \tag{A3}$$

where the first case corresponds to the quadratic-energy-dependent Green's function retained here and the second case to the linear one. After some algebra, it is found that in the large-t' limit and for a negligible pion mass, the integral with the first integrand becomes

$$\begin{aligned} I_{56}(t'\to\infty) &\simeq -\frac{1}{2} I_{75}(t'\to\infty) \\ &\simeq \frac{\tilde{K}}{M\sqrt{t'}}\left[\frac{t'}{2M^2} - \frac{1}{8}\ln\left(\frac{t'}{M^2}\right) + \frac{1}{8} - \frac{1}{2}\ln(2)\right]. \end{aligned} \tag{A4}$$

The absence of the intermediate term $1/(M^2)$ results from a nontrivial cancellation. All the other terms not considered here behave like $1/(M\sqrt{t'})$ (up to log terms) for the most important ones. It can thus be checked that the contributions of order $\sqrt{t'}/M^3$ to the spectral functions $g_{56}(t')$ and $g_{75}(t')$ cancel, leaving contributions of order $1/(M\sqrt{t'})$.

Had we used the other Green's function, the dominant contribution resulting from performing the integral would read

$$I_{56}(t'\to\infty) \simeq -\frac{1}{2} I_{75}(t'\to\infty) \simeq \tilde{K}\frac{\sqrt{t'}}{2M^3}\frac{2+\pi}{4}, \tag{A5}$$

and the corresponding $g(t')$ functions would be given by

$$g_{56}(t'\to\infty) \simeq -\frac{1}{2} g_{75}(t'\to\infty) \simeq \tilde{K}\frac{\sqrt{t'}}{2M^3}\frac{\pi-2}{4}. \tag{A6}$$

Thus, in contrast to the quadratic-energy-dependent Green's function, no cancellation of the dominant terms is found with the consequence that the dispersion integrals involving the spectral functions $g_{56}(t')$ and $g_{75}(t')$, Eqs. (5), do not converge (logarithmic divergence). Moreover, these functions evidence a sign change around $t' = 20$–25 GeV^2. Actually, this has little effect on the spectral functions at low values of t' but, of course, this prevents one from getting convergent results. The sensitivity of the configuration-space potentials did not exceed 10% at $r = 1$ fm [15].

APPENDIX B: PARITY-VIOLATING TWO-PION EXCHANGE NN POTENTIAL FROM EFFECTIVE FIELD THEORY

In this Appendix, we give the details of the momentum-space contributions from the TPE diagrams shown in Fig. 2, employing a heavy-baryon chiral Lagrangian and the dimensional regularization in the d-dimensional space-time, $d = 4 - 2\epsilon$.

From diagrams (b), (c), and (d), we get

$$\begin{aligned} V_{(b)} &= -i(\vec{\tau}_1\times\vec{\tau}_2)^z(\vec{\sigma}_1+\vec{\sigma}_2)\cdot\vec{q}\,\frac{\pi g_A h_\pi^1}{\sqrt{2}(4\pi f_\pi)^3} \\ &\quad \times\left[\frac{1}{\epsilon} - \gamma + \ln(4\pi) + \ln\left(\frac{\mu^2}{m_\pi^2}\right) + 2 - 2L(q)\right], \end{aligned} \tag{B1}$$

$$\begin{aligned} V_{(c)} &= -i(\vec{\tau}_1+\vec{\tau}_2)^z(\vec{\sigma}_1\times\vec{\sigma}_2)\cdot\vec{q}\,\frac{2\sqrt{2}\pi g_A^3 h_\pi^1}{(4\pi f_\pi)^3} \\ &\quad \times\left[\frac{1}{\epsilon} - \gamma + \ln(4\pi) + \ln\left(\frac{\mu^2}{m_\pi^2}\right) + 2 - 2L(q)\right] \\ &\quad - i(\vec{\tau}_1\times\vec{\tau}_2)^z(\vec{\sigma}_1+\vec{\sigma}_2)\cdot\vec{q}\,\frac{\sqrt{2}\pi g_A^3 h_\pi^1}{2(4\pi f_\pi)^3} \end{aligned}$$

$$\times \left\{ -\frac{3}{2}\left[\frac{1}{\epsilon} - \gamma + \ln(4\pi) + \ln\left(\frac{\mu^2}{m_\pi^2}\right) + \frac{4}{3}\right] + 3L(q) - H(q)\right\}, \tag{B2}$$

$$V_{(d)} = -i(\vec{\tau}_1 \times \vec{\tau}_2)^z (\vec{\sigma}_1 + \vec{\sigma}_2)\cdot\vec{q}\,\frac{\sqrt{2}\pi g_A^3 h_\pi^1}{2(4\pi f_\pi)^3} \times \left\{ -\frac{3}{2}\left[\frac{1}{\epsilon} - \gamma + \ln(4\pi) + \ln\left(\frac{\mu^2}{m_\pi^2}\right) + \frac{4}{3}\right] + 3L(q) - H(q)\right\}, \tag{B3}$$

where $L(q)$ and $H(q)$ are defined in Eq. (13), and the Euler number is given by $\gamma = 0.5772\cdots$. The quantity μ represents the scale of the dimensional regularization, and $q = |\vec{q}|$ with $\vec{q}$ defined by Eq. (2). We note that we have employed, in the calculation of diagram (d), the same prescription to subtract the two-nucleon-pole contribution as in Ref. [6] [Eq. (C.3)].

All these potentials from the loop diagrams have infinities (i.e., the $1/\epsilon$ terms). Along with the finite constant terms, they are renormalized by the counter terms (PV NN contact terms) $\tilde{C}_2 + \tilde{C}_4$ and C_6 (see Eq. (5) in Ref. [6]). In the MX scheme, the $L(q)$ and $H(q)$ terms, which are the only ones to contribute to the finite-range potential, are retained. This procedure fixes the associated contact term. In the $\overline{\text{MS}}$ scheme, besides $L(q)$ and $H(q)$ terms, an extra term, $\ln(\mu^2/m_\pi^2) + 2$, (written as $2[1 + \ln(\mu/m_\pi)]$ in the main text), which produces a contact term, appears.

[1] C. Ordoñez, L. Ray, and U. van Kolck, Phys. Rev. C **53**, 2086 (1996).
[2] E. Epelbaum, W. Glöckle, and U.-G. Meißner, Nucl. Phys. **A671**, 295 (2000).
[3] D. R. Entem and R. Machleidt, Phys. Rev. C **68**, 041001 (2003).
[4] For a recent review, see, for example, E. Epelbaum, Prog. Part. Nucl. Phys. **57**, 654 (2006), and references therein.
[5] S. Weinberg, Phys. Lett. **B251**, 288 (1990); Nucl. Phys. **B363**, 3 (1991).
[6] S.-L. Zhu, C. M. Maekawa, B. R. Holstein, M. J. Ramsey-Musolf, and U. van Kolck, Nucl. Phys. **A748**, 435 (2005).
[7] G. S. Danilov, Sov. J. Nucl. Phys. **14**, 443 (1972).
[8] J. Missimer, Phys. Rev. C **14**, 347 (1976).
[9] B. Desplanques and J. Missimer, Nucl. Phys. **A300**, 286 (1978).
[10] C. H. Hyun, S. Ando, and B. Desplanques, Phys. Lett. **B651**, 257 (2007).
[11] C.-P. Liu, Phys. Rev. C **75**, 065501 (2007).
[12] D. Pignon, Phys. Lett. **B35**, 63 (1971).
[13] B. Desplanques, Phys. Lett. **B41**, 61 (1972).
[14] H. Pirner and D. O. Riska, Phys. Lett. **B44**, 151 (1973).
[15] M. Chemtob and B. Desplanques, Nucl. Phys. **B78**, 139 (1974).
[16] N. Kaiser, Phys. Rev. C **76**, 047001 (2007).
[17] Y.-R. Liu and S.-L. Zhu, arXiv:0711.3838.
[18] J. A. Niskanen, T. M. Partanen, and M. J. Iqbal, arXiv:0712.2399.
[19] B. Desplanques, Nucl. Phys. **A242**, 423 (1975).
[20] C. H. Hyun, B. Desplanques, S. Ando, and C.-P. Liu, arXiv:0802.1606.
[21] R. Higa, M. R. Robilotta, and C. A. da Rocha, Nucl. Phys. **A790**, 384 (2007).
[22] S. I. Ando and H. W. Fearing, Phys. Rev. D **75**, 014025 (2007).
[23] A. Amghar, B. Desplanques, and L. Theußl, Nucl. Phys. **A714**, 213 (2003).
[24] S. A. Coon and J. L. Friar, Phys. Rev. C **34**, 1060 (1986).
[25] M. Lacombe *et al.*, Phys. Rev. C **21**, 861 (1980).
[26] G. Barton, Nuovo Cimento **19**, 512 (1961).
[27] S. L. Adler, Phys. Rev. **140**, B736 (1965); W. I. Weisberger, *ibid.* **143**, 1302 (1966).
[28] B. Desplanques, J. F. Donoghue, and B. R. Holstein, Ann. Phys. (NY) **124**, 449 (1980).
[29] B. R. Holstein, Phys. Rev. D **23**, 1618 (1981).
[30] N. Kaiser and U.-G. Meissner, Nucl. Phys. **A499**, 727 (1989).
[31] B. Desplanques, Phys. Rep. **297**, 1 (1998).
[32] S. Kistryn *et al.*, Phys. Rev. Lett. **58**, 1616 (1987).
[33] P. D. Eversheim *et al.*, Phys. Lett. **B256**, 11 (1991).
[34] A. R. Berdoz *et al.*, Phys. Rev. Lett. **87**, 272301 (2001).
[35] J. S. Nico and W. M. Snow, Annu. Rev. Nucl. Part. Sci. **55**, 27 (2005).
[36] R. B. Wiringa, V. G. J. Stoks, and R. Schiavilla, Phys. Rev. C **51**, 38 (1995).
[37] M. Simonius, Phys. Lett. **B41**, 415 (1972); Nucl. Phys. **A220**, 269 (1974).
[38] R. Machleidt, Phys. Rev. C **63**, 024001 (2001).
[39] V. G. J. Stoks, R. A. M. Klomp, C. P. F. Terheggen, and J. J. deSwart, Phys. Rev. C **49**, 2950 (1994).
[40] A. Amghar and B. Desplanques, Nucl. Phys. **A714**, 502 (2003).
[41] B. Desplanques, Phys. Lett. **B512**, 305 (2001).
[42] C. H. Hyun, T.-S. Park, and D.-P. Min, Phys. Lett. **B516**, 321 (2001).